

# New Vacuum Tube and Output Transformer Models applied to the Quad II valve amplifier

Menno van der Veen; ir.buro Vanderveen; The Netherlands; mennovdv@noord.bart.nl  
Pierre Touzelet; 76 rue Lavoisier, Vélizy; 78140 France; p.touzelet@sereme.com

**Abstract - In earlier preprints new vacuum tube and output transformer equivalent models were proposed. These models are now applied to the famous Quad II valve amplifier. Results of models and measurements are compared in the frequency-time and amplitude domains. It is demonstrated that output transformers and multi grid vacuum tubes and complete vacuum tube amplifiers can be modeled with great precision**

## 1. INTRODUCTION

In earlier work (1) an equivalent model was introduced for toroidal output transformers for push-pull vacuum tube amplifiers. In preprint (2) a generalized push-pull vacuum tube model was introduced based on a modified Child-Langmuir equation. Small signal analysis techniques were introduced in (3), based on a systematic use of Taylor's expansions.

In this preprint we demonstrate the validity and applications of the models with the valve amplifier "The Quad II", designed by Sir Peter J. Walker. This amplifier is well known and available worldwide. It is an excellent example to demonstrate our new models and theories.

Chapter 2 discusses the general concept of the Quad II amplifier, the measurements on the original output transformer and the characteristic quantities which need to be known to model this transformer. Chapter 3 describes the KT66 vacuum tubes, used in the power section of the amplifier. They are characterized by five parameters of the modified Child-Langmuir equation. Chapter 4 compares results of the models and measurements in the frequency-time domain for the complete amplifier with and without overall negative voltage feedback. The maximum output power and the complex character of the amplifiers output impedance are discussed in detail. Chapter 5 discusses models and measurements in the amplitude domain, investigating distortions.

In general: the agreement between "theory" and "practice" is striking. This work delivers a new alternative approach to modeling techniques as used in PSpice (4-7) and special dedicated Matlab programs that are presently available on the internet (8). The vacuum tube amplifier technology is very alive nowadays, especially in so called "high-end" audio amplifiers. Modern computer calculation techniques are intensively applied to new vacuum tube amplifier

designs. Most available vacuum tube models describe very well the behavior of triodes, while our models are applicable to triodes and also to multi-grid vacuum tubes, like tetrodes and pentodes.

## 2. SCHEMATICS AND MODELLING THE OUTPUT TRANSFORMER

### 2.1 Schematic diagram

Figure 2.1 shows the schematic diagram of the Quad II valve amplifier. It comprises an input section with two EF86 tubes for pre-amplification and phase splitting. The power section uses two auto biased KT66 tubes. The push-pull output transformer has separate cathode feedback windings and a multi tapped secondary for various loudspeaker impedance's. The amplifier delivers 15 Watt output power. Different voltages and currents are clearly indicated in the schematics.

### 2.2 Output transformer parameters

By means of voltage ratio measurements at 1 kHz the turns ratios of the different windings of the output transformer are determined:

$$\begin{aligned}N_{Z-X} / N_{P-Q} &= 27.92 \\N_{U-W} / N_{P-Q} &= 3.16 \\N_{T-P} / N_{P-Q} &= 2.0 \\N_{S-R-P} / N_{P-Q} &= 1.5\end{aligned}$$

According to the original Quad II specifications, the recommended optimal loudspeaker impedance between the taps S=R and P is  $Z_L = 7$  ohm, meaning that the total primary impedance between Z and X equals:

$$Z_{aa} = 2425 \text{ ohm.}$$

The maximum value of the primary inductance is measured with a 50 Hz sinusoidal voltage of 180 V<sub>rms</sub>:

$$L_{p,max} = 122 \text{ H}$$

The DC resistances of the total primary winding Z-X and the secondary winding P-Q are given by:

$$\begin{aligned}R_{ip} &= 304 \text{ ohm} \\R_{is} &= 0.8 \text{ ohm}\end{aligned}$$

With the frequencies for impedance resonance the primary to secondary leakage inductance  $L_{sp}$  and the

effective internal primary capacitance  $C_{ip}$  are determined:

$$\begin{aligned} L_{sp} &= 6.4 \text{ mH} \\ C_{ip} &= 467 \text{ pF} \end{aligned}$$

The parameters given above determine the behavior of the output transformer in the frequency domain for a speaker load of 7 ohm, as explained in full detail in (1).

### 3 MODELLING THE KT66

#### 3.1 Handbook parameter set

Tube handbooks deliver information about the KT66. The following set of data is used:

$$\begin{aligned} S &= 6.3 \text{ mA/V} \\ r_p &= 22.5 \text{ kohm} \\ I_{a0} &= 85 \text{ mA} \\ I_{g20} &= 6.3 \text{ mA} \\ V_{ak0} &= V_{g20} = 250 \text{ V} \\ V_{g10} &= -14.6 \text{ V} \end{aligned}$$

#### 3.2 Five parameter set

According to the procedures as described in (2), the five parameter set of the KT66 is calculated, resulting in:

$$\begin{aligned} [n; \alpha_o; K; D_a; D_{g2}] &= \\ [10; 0.966; 1.003 \cdot 10^{-3}; 3.619 \cdot 10^{-3}; 0.136] \end{aligned}$$

The Child-Langmuir equation with its modification  $\alpha$  that belongs to the five parameter-set is given below:

$$\begin{aligned} \alpha &= \frac{I_a}{I_k} = \alpha_o \left[ \frac{2}{\pi} \text{Arctg} \left( \frac{V_{ak}}{V_{g2k}} \right) \right]^{1/n} \\ I_a &= \alpha K (V_{g1k} + D_{g2} V_{g2k} + D_a V_{ak})^{\frac{3}{2}} \end{aligned} \quad (3.2.1)$$

#### 3.3 Initial test of the new parameter set

A quick initial test is possible about the validity of the equation 3.2.1 plus the five parameter set, by using the voltages and currents in the quiescent operating point as given in the schematic diagram of the Quad II amplifier. The voltage at the cathode (tap V) equals  $V_{k0} = 26 \text{ V}$ . Then  $V_{ak0} = 340 - 26 = 314 \text{ V}$  and  $V_{g2k0} = 330 - 26 = 304 \text{ V}$ . The anode current equals  $I_{a0} = 65 \text{ mA}$ . With formula 3.2.1 the control grid voltage  $V_{g1k0}$  can be calculated:  $V_{g1k0} = -25,2 \text{ V}$ , which only deviates 3% of  $V_{k0} = 26 \text{ V}$ . Because  $[I_{k0} = I_{a0} + I_{g20}]$  the calculated screen grid current equals  $I_{g20} = 7 \text{ mA}$  as shown in the diagram.

### 4 SMALL SIGNAL TRANSFER FUNCTION

#### 4.1 Effective plate resistance of the KT66

Through the cathode windings at the output transformer

an amount  $\Gamma = N_{U-w} / N_{Z-X} = 0.11$  of negative voltage feedback is applied at the cathode of each KT66. In the Quad II circuit there is no feedback at the screen grids, so  $X = 0$ . Using the new coupling model of (2), the effective plate resistance of each KT66 tube can be calculated, resulting in:

$$r_{p,\text{eff}} = 2 r_{i,\text{eff}} = 1171 \text{ ohm}$$

The total primary winding of the output transformer is driven by two tubes. In (2) this circuit is represented by a single voltage source with an effective generator resistance  $R_{\text{gen,eff}}$  driving the total primary winding, with

$$R_{\text{gen,eff}} = 2 r_{p,\text{eff}} = 2342 \text{ ohm}$$

Again a quick initial test of this result is possible, by calculating and measuring at 1 kHz the output impedance  $Z_{\text{out}}$  at the speaker terminals, when no overall negative voltage feedback is applied (R11 is temporally removed):

$$Z_{\text{out}} = \left[ \frac{N_{S-P}}{N_{Z-X}} \right]^2 \cdot (R_{\text{gen,eff}} + R_{ip}) + R_{is} \quad (4.1.1)$$

The calculated value of  $Z_{\text{out}}$  equals 8.5 ohm, while the measured value is 7.9 ohm (at 1 kHz sine wave and 2.8  $V_{\text{rms}}$  at speaker terminals). These values differ 6.7%, which is considered to be a negligible difference, taking aging and deviations in specifications of tubes into account.

Looking more precise into this, there appears to be another effect. Using the Tailor expansions of (3), the value of  $r_{i,\text{eff}}$  can be calculated as function of the alternating voltage at the control grids of the KT66 tubes. Figure 4.1 shows the result. At higher alternating voltages the generator resistance becomes larger, which easily can be explained considering the descending slope of the  $I_a$ - $V_{ak}$  characteristics of the KT66 tube at higher control grid voltages.

#### 4.2 Transfer Function of power section

In (1) is explained how to calculate the transfer function of the two KT66 tubes combined with the output transformer. The primary inductance  $L_{p,\text{max}}$  of the transformer, combined with the effective plate resistance of the tubes create a first order high pass filter with -3dB frequency  $f_{-3L}$ :

$$f_{-3L} = 1.55 \text{ Hz}$$

At high frequencies  $L_{sp}$  and  $C_{ip}$  create a second order low pass filter with central frequency  $f_o$  and Q-factor:

$$\begin{aligned} f_o &= 131 \text{ kHz} \\ Q &= 1 / a_2 = 0.664 \end{aligned}$$

The normalized transfer function  $H_1(f)$  of the KT66 tubes and the output transformer is shown in formula 4.2.1 ( $j = \text{sqrt}(-1)$ ):

$$H_1(f) = \frac{jf}{jf + f_{-3L}} \cdot \frac{1}{1 + \frac{1}{Q} \cdot \frac{jf}{f_o} + \left(\frac{jf}{f_o}\right)^2} \quad (4.2.1)$$

#### 4.3 Transfer Function of the EF86 section

The input-driver section with the two EF86 tubes contains two filters. The first is a high pass filter, first order, created by the coupling capacitors C2 and C3 plus the resistors R7 and R9. Its -3dB frequency is given by:

$$f_{C2,3-L} = 1.85 \text{ Hz}$$

The second filter is created by the 'large' output impedance of the EF86 tubes and their 'large' anode resistances R5 and R6, combined with the Miller capacitance's at the control grids of the KT66 power tubes. Its -3dB first order low pass frequency is given by:

$$f_{EF86-H} = 7.5 \text{ kHz}$$

The normalized transfer function  $H_2(f)$  of the EF86 section is given in formula 4.3.1.

$$H_2(f) = \frac{jf}{jf + f_{C2,3-L}} \cdot \frac{f_{EF86-H}}{jf + f_{EF86-H}} \quad (4.3.1)$$

#### 4.4 Transfer Function of the complete amplifier

Without feedback in the amplifier (R11 temporarily removed) and without a loudspeaker connected to the speaker terminals, the voltage amplification  $A_0$  at 1 kHz is measured from input to output:

$$A_0 = 100$$

The transfer function  $A_0(f)$  of the total amplifier, unloaded at the output, is given by formula 4.4.1 and shown in the upper curve of figure 4.4.1:

$$A_0(f) = A_0 \cdot H_1(f) \cdot H_2(f) \quad (4.4.1)$$

With R11 connected, the effective feedback factor  $\beta$  with respect to the 7 ohm tap S=R is given by:

$$\beta = N_{P-Q} / N_{P-S} R_{10} / (R_{10} + R_{11}) \\ \beta = 0.117$$

The effective transfer function of the complete amplifier, with negative voltage feedback and loaded by

a loudspeaker  $Z_L$  is given by formula 4.4.2:

$$A_{eff,L}(f) = \frac{A_0(f)}{1 + \beta \cdot A_0(f)} \cdot \frac{Z_L}{\frac{Z_{out}}{1 + \beta \cdot A_0(f)} + Z_L} \quad (4.4.2)$$

The two lower curves in figure 4.4.1 show the result of the calculation with formula 4.4.2 and the measurement with  $Z_L = 7 \text{ ohm}$ . The agreement is striking. Only at the highest frequencies some partial resonance's appear in the EI-core output transformer of the Quad II amplifier, which are no part of the modeling of a toroidal core output transformer in (1).

The calculated transfer at low frequencies with feedback shows a maximum while the measurements show a gentle roll off, see figure 4.4.1. This deviation can be explained with the assumption that is made in the calculation:

The frequency  $f_{-3L}$  is calculated with the maximum value  $L_{P,max}$ . However, at small and moderate AC output levels, the actual value of  $L_P$  will be smaller (up to 10 times) than  $L_{P,max}$ . Consequently  $f_{-3L}$  will be larger than the given value of 1.55 Hz. Implementing such a larger  $f_{-3L}$  value into the calculation causes the maximum to disappear. Then measurements and calculation are in full agreement again. See figure 4.4.2.

There is one peculiar condition where this maximum can be noticed: "switch the amplifier off while listening to music". Then the sound level will decrease 'swinging' in loudness with a swing-frequency equal to the frequency of the calculated maximum. But who listens to an amplifier while switching the power off?

#### 4.5 Output impedance

The output impedance  $Z_{out,eff}$  of the complete amplifier at a small signal output level is given by formula 4.4.3.

$$Z_{out,eff}(f) = \frac{Z_{out}}{1 + \beta \cdot A_0(f)} \quad (4.4.3)$$

This formula shows that this output impedance is a complex function, therefore  $|Z_{out,eff}(f)|$  is shown in figure 4.5.

#### 4.6 Voltages, Currents and Powers

Figure 4.6.1 shows the calculated anode and screen grid currents per KT66 tube as function of the momentary anode voltage. With these data the output power  $P_{out}$ , the anode dissipation  $P_a$  and the screen grid dissipation  $P_{g2}$  can be calculated as function of the alternating control grid voltage. The results are shown in figure 4.6.2. The calculations show a maximum output power

of 18 W, while 15 W is measured. The difference can be explained and calculated taking the transformer winding resistances  $R_{ip}$  and  $R_{is}$  into account, which cause insertion loss inside the output transformer.

## 5 DISTORTIONS

### 5.1 Harmonic distortions without feedback

In (3) the procedure is explained how to calculate harmonic distortions, using the Taylor expansions. Figure 5.1 shows the results of the calculated distortions at 1 kHz only in the section of KT66 tubes plus output transformer. No overall feedback is applied nor any influence of the EF86 vacuum tubes nor transformer distortions are taken into account. It is striking that there is no 2nd harmonic distortion, which is a direct consequence of the push-pull concept.

### 5.2 Harmonic distortions with feedback

Applying overall negative feedback, the THD-figures of figure 5.1 get smaller by the factor of  $1 / (1 + \beta A_0)$ . Figure 5.2 shows the calculated results plus measured harmonic distortions at the actual amplifier.

The second harmonic distortion is not zero, as calculated. The measured third harmonic distortion appears to be 10 times larger than the calculated distortion.

These deviations mainly are caused by not modeling the EF86 circuitry nor taking output transformer behavior into account.

The EF86 circuit can be modeled in the same way as the KT66 vacuum tubes, however was not done in this preprint.

The output transformer distortions are subject of present research and modeling, taking the real dynamic B-H relation of actual cores into account.

In general about distortions: only if the complete amplifier is modeled, real calculations can be performed with better precision. At this moment we are not ready to show such results.

## 6 CONCLUSIONS

The output transformer of a push-pull vacuum tube amplifier can be modeled with a simple equivalent circuit as proposed in (1).

A multi grid vacuum tube can be modeled with the modified Child-Langmuir equation as proposed in (2) and (3). The model replaces the vacuum tubes in a push-pull amplifier by an equivalent circuit, consisting of a single voltage source with series generator resistance. This resistance appears to be not constant and depends on the momentary voltages at the tube.

The output impedance of a push-pull amplifier can be calculated taking vacuum tube generator resistance and output transformer specifications into account. There is good agreement between calculations and measurement. In the frequency domain the transfer function of modeled tubes and output transformer can be calculated

with good precision. Only small partial high frequency resonance's are not modeled.

The established theories of overall negative voltage feedback are proven once again in this work.

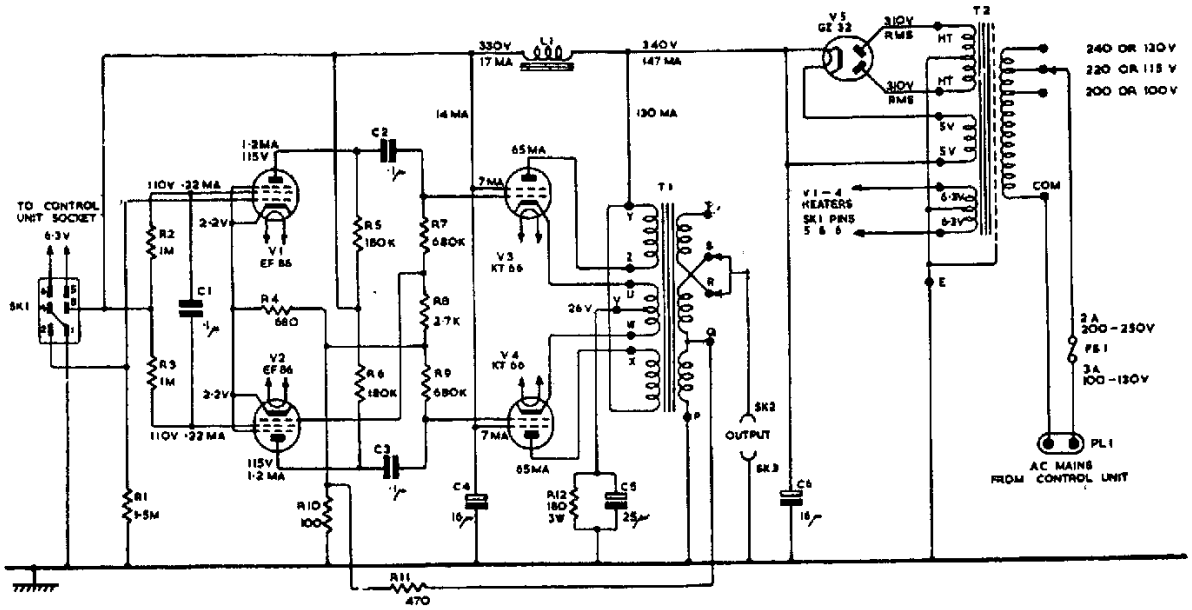
The new vacuum tube and output transformer models allow precise calculation of amplifiers output power, power loss inside the output transformer, as well as heat dissipations at screen grid and anode of each power tube.

Harmonic distortions of a complete push-pull vacuum tube amplifier can be calculated, although this procedure has not yet been completed. Especially a new model of the output transformer needs further work, taking real B-H behavior inside the core into account.

It really is amazing, after so many years of the design date of the Quad II amplifier (approx. 1950), to notice that present computer modeling again proves the excellent and sound qualities of this famous amplifier.

## 7 REFERENCES

- 1: **Menno van der Veen**: "Theory and Practice of Wide Bandwidth Toroidal Output Transformers"; preprint 3887, AES convention 1994 November San Francisco
- 2: **Menno van der Veen**: "Modeling Power Tubes and their Interaction with Output Transformers"; preprint 4643, AES convention 1998 May Amsterdam
- 3: **Pierre Touzelet**, Menno van der Veen: "Small Signal Analysis for generalized push-pull tube amplifier topology"; preprint 5587, AES convention 2002 May Munich
- 4: **W. Marshall Leach Jr.**: "Spice models for vacuum-tube amplifiers"; JAES Vol 43/3; 1995 March
- 5: **Scott Reynolds**: "Vacuum-tube models for Pspice simulations"; Glass Audio; Vol 5/4 1993
- 6: **Eric Pritchard**: "Tube model critique"; Glass Audio; Vol 8/1 1996
- 7: **Norman Koren**: "Improved Vacuum-tube models for Spice simulations"; Glass Audio; Vol 8/5 1996
- 8: **Eugene V. Karpov**: good starting address for internet search: [www.next-power.net/next-tube.html](http://www.next-power.net/next-tube.html)



DRG 11175, ISSUE 1. THE VOLTAGE AND CURRENT MEASUREMENTS SHOWN ARE APPROXIMATE, AND ARE ONLY PROVIDED AS A GUIDE. ALLOWANCE SHOULD BE MADE FOR THE LOADING EFFECTS OF A VOLTMETER.

Figure 2.1: Schematic Diagram of the Quad II Valve Amplifier

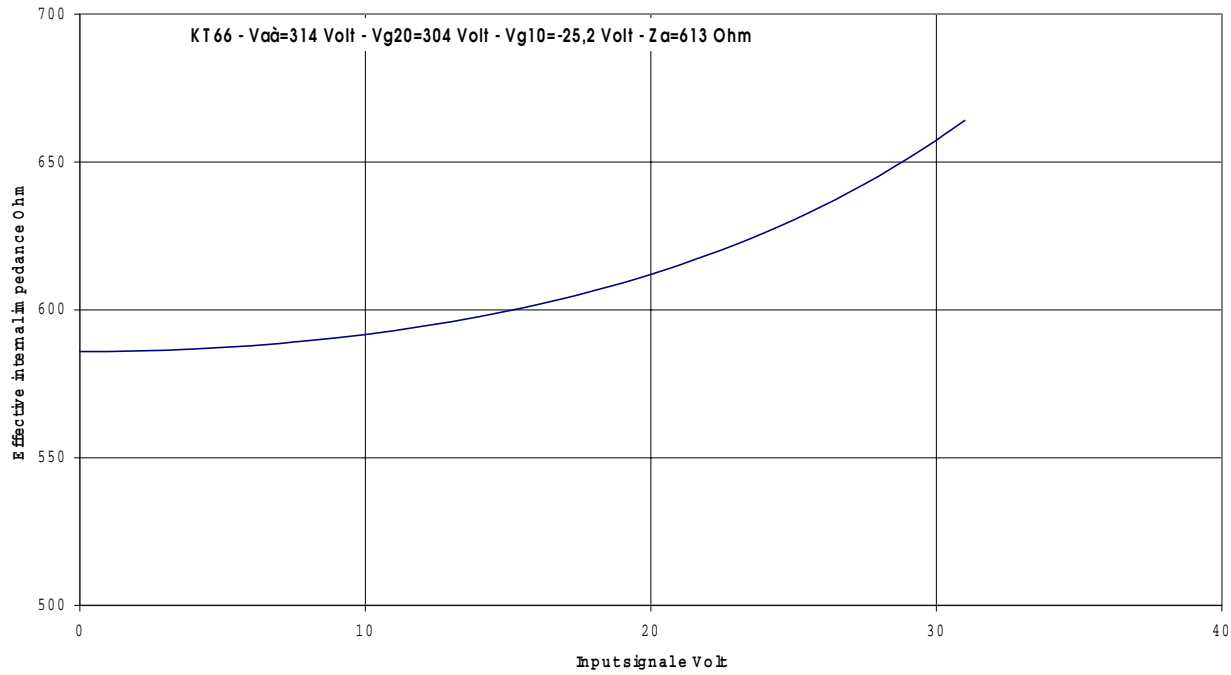


Figure 4.1: Effective impedance  $r_{i,eff}$  as function of the alternating KT66 control grid voltage

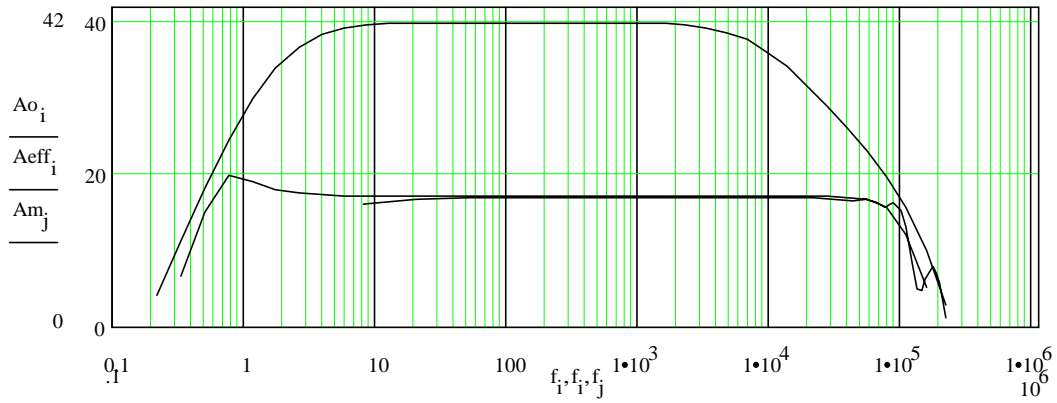


Figure 4.4.1: Transfer functions in dB: upper curve is the calculation without NFB; lower curves are measurements and calculation with NFB

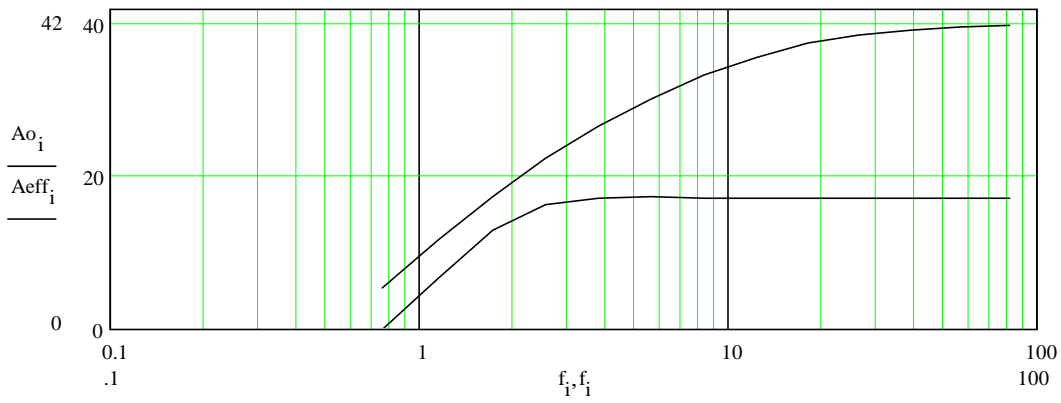


Figure 4.4.2: Transfer function in dB: upper curve is calculation without NFB for  $L_{p,max} = 12,2$  H; the lower curve is calculated with NFB.

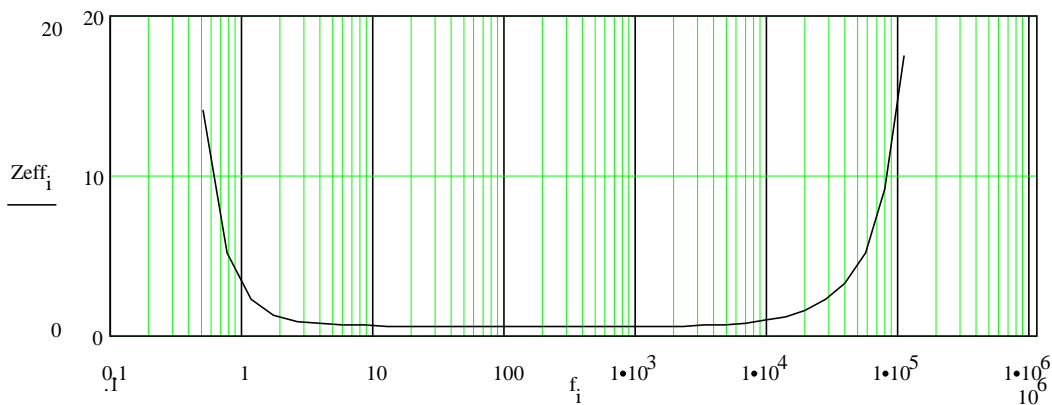


Figure 4.5: Effective output impedance (absolute value) of the amplifier with NFB for  $L_p = L_{p,max}$ .

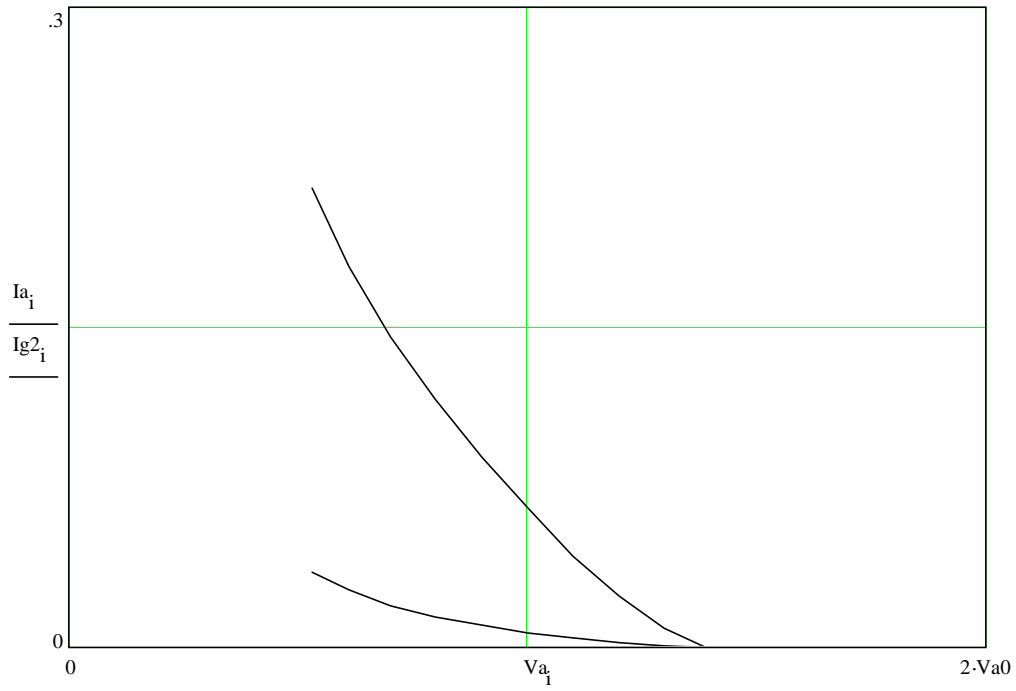


Figure 4.6.1: Anode current (upper curve) and Screen Grid Current (lower curve) per KT66 as function of the momentary anode voltage. The middle of the x-axis is the quiescent operating point.

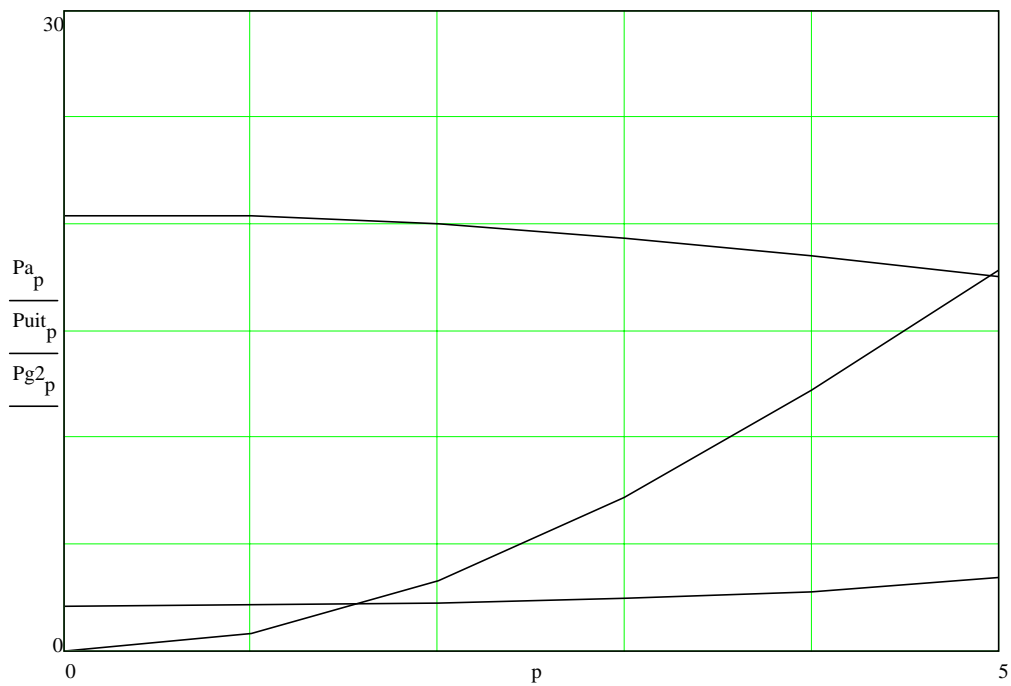


Figure 4.6.2: Anode dissipation per KT66 (upper curve); output power (middle curve); screen grid dissipation per KT66 (lower curve), as function of the control grid voltage (arbitrary unit)

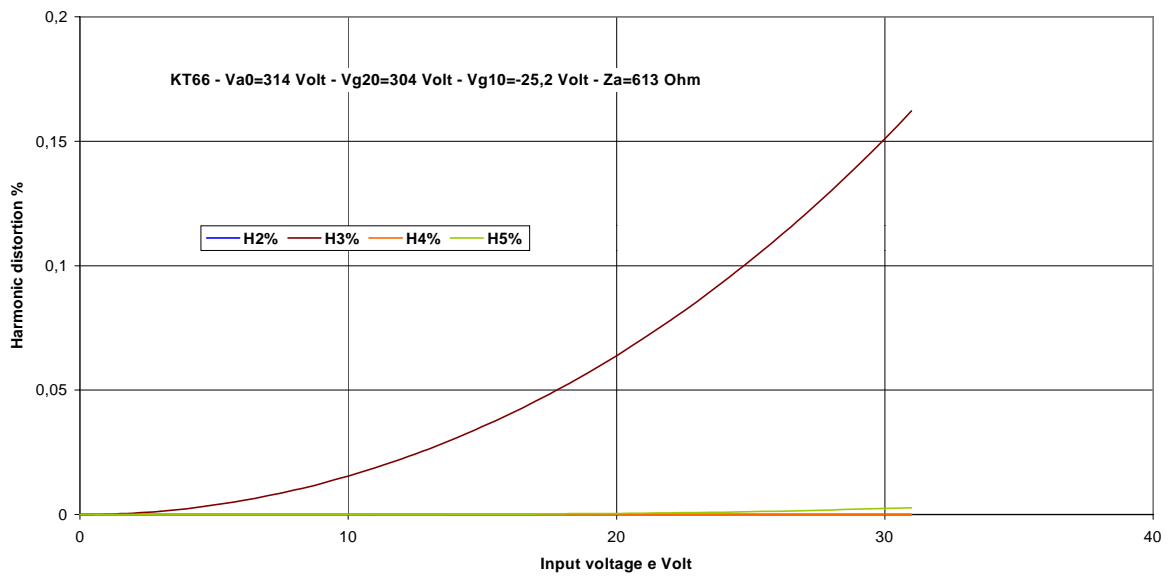


Figure 5.1: Calculated harmonic distortions in KT66's plus OPT section assuming no THD in the OPT and no NFB

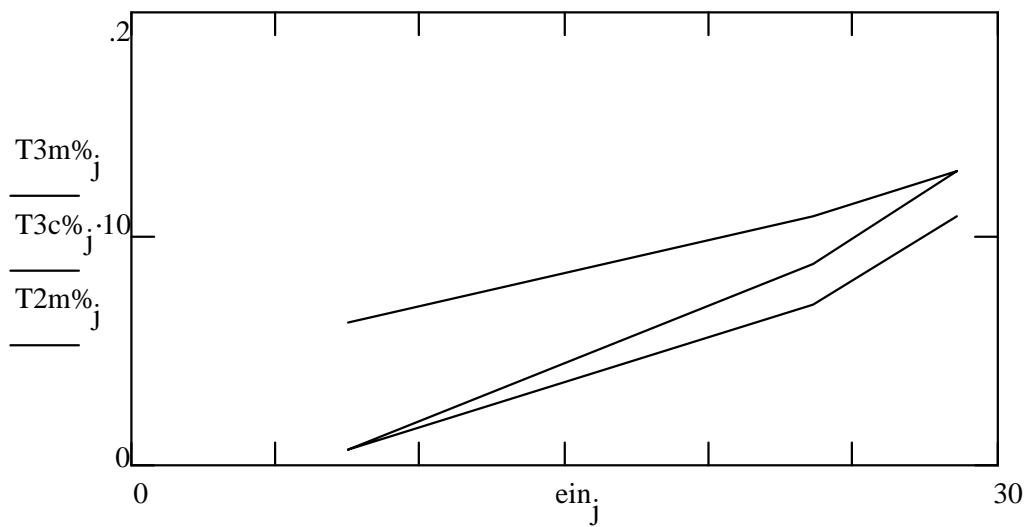


Figure 5.2: Harmonic Distortion (%) at 1kHz as function of the KT66 control grid voltage with overall negative feedback:  
 2-nd harmonic distortion (measured, upper curve);  
 3-rd harmonic distortion (measured, 2-nd curve);  
 3-rd harmonic distortion times 10 (calculated, 3-rd curve).